

isotopes are shown in Fig. 15 and indicate the possibility that the spin of Ti^{43} is $\frac{3}{2}^+$ should this systematic trend be continued. This, however, appears unlikely in view of the most probable spin assignment for its mirror nucleus Sc^{43} as $J^\pi = \frac{7}{2}^-$.²³

Finally, energy level diagrams showing l_n values, angular momenta, and parities of the levels observed in Ti^{49} , Ti^{48} , Ti^{47} , Ti^{46} , and Ti^{45} in the present (p, d) investigation are shown in Fig. 16.

CONCLUSIONS

The present investigation has shown that for the Ti isotopes, many of the important features of the (p, d) reaction to low-lying levels are well explained under the assumption that neutrons and protons in excess of 20 are in a $(1f_{7/2})^n$ configuration, and that attempts to treat the spectra in terms of only neutron configuration (assuming the protons to be coupled to 0)

²³ T. Lindquist and A. C. G. Mitchell, Phys. Rev. **95**, 1535 (1954).

are inadequate. The next step in the calculation is to add $2p$ admixture, actually only $2p_{3/2}$ as no evidence was found for $2p_{1/2}$ admixture. The fact that some even parity levels appear to go by a direct reaction process in both pickup and stripping reactions is of great interest. The conclusion reached here that this effect reflects admixture from the lower lying $2s_{1/2}$ and $1d_{3/2}$ shells follows logically from the experimental results, but one may wish to question whether the knowledge of the reaction mechanism is sufficient to allow such conclusions about initial and final states.

ACKNOWLEDGMENTS

We wish to thank Professor B. F. Bayman, Professor J. D. McCullen, and Professor R. Sherr for their interest in, and discussions of the investigation. We also wish to thank Dr. L. Zamick for his helpful comments, and to acknowledge the help we have obtained from Dr. E. Rost in the DWBA calculation. We are grateful to Dr. J. Rapaport for communicating to us a copy of his thesis prior to publication.

Isomer Ratios from (α, xn) Reactions on Silver*

C. T. BISHOP† AND J. R. HUIZENGA
Argonne National Laboratory, Argonne, Illinois

AND

J. P. HUMMEL
University of Illinois, Urbana, Illinois
(Received 2 March 1964)

Excitation functions have been measured for the $Ag^{107}(\alpha, n)In^{110,110m}$ and $Ag^{109}(\alpha, 3n)In^{110,110m}$ reactions with isotopically separated targets. The excitation functions for the high-spin metastable state peak in both reactions at higher bombarding energies than the low-spin ground state. In the case of the $Ag^{107}(\alpha, n)$ reaction, the cross section for the formation of In^{110} peaks at a helium-ion energy of about 17 MeV and that for In^{110m} peaks at about 19.5 MeV. The isomer ratio, $\sigma_m/(\sigma_m + \sigma_g)$, determined for the $Ag^{107}(\alpha, n)$ reaction varies from 0.13 at a helium-ion energy of 10.8 MeV to 0.81 at a helium-ion energy of 22.0 MeV. In the $Ag^{109}(\alpha, 3n)$ reaction, this ratio varies from 0.68 at a helium-ion energy of 27.6 MeV to 0.87 at a helium-ion energy of 38.7 MeV. The experimental cross sections are based on measured half-lives of 70.2 ± 1.4 min and 5.2 ± 0.2 h for In^{110} and In^{110m} , respectively. The isomer ratios were calculated theoretically for the above reactions and the effects of various parameters on the calculations were examined. The experimental isomer ratios for the $Ag^{107}(\alpha, n)$ reaction for bombarding energies below 18 MeV agree within experimental uncertainties with calculated results based on either a Fermi-gas model with a rigid moment of inertia ($\sigma^2 = 34.7t$) or a superconductor model. A superconductor model predicts only about a 20% reduction in the moment of inertia for In^{110} and such a small change could not be definitely established from the data. A marked increase in the experimental isomer ratios from the $Ag^{107}(\alpha, n)$ reaction is observed near the onset of the ($\alpha, 2n$) reaction. This increase is probably due to a fractionation of the intermediate spin distribution for energies slightly exceeding the threshold of a second reaction. This effect is suggested also in the $Ag^{109}(\alpha, 3n)$ reaction by the small experimental isomer ratios at bombarding energies where the ($\alpha, 2n$) competition is sizeable. These results indicate that values of σ deduced from the isomer ratio technique are in error at energies where cross sections for a competing reaction are large.

I. INTRODUCTION

IN this investigation angular momentum effects in the $Ag^{107}(\alpha, n)$ and $Ag^{109}(\alpha, 3n)$ reactions at several helium-ion bombarding energies have been studied by

* This paper is based in part on a thesis submitted to the faculty of the University of Illinois by Carl T. Bishop in partial fulfill-

ment of the requirements for the degree of Doctor of Philosophy, 1961. This work was performed under the auspices of the U. S. Atomic Energy Commission.

† Present address: Villa Madonna College, Covington, Kentucky.

the ratio of the cross section for the formation of the high-spin isomer to the total cross section, $\sigma_m/(\sigma_m+\sigma_g)$. The study of the $\text{In}^{110,110m}$ isomers from the $\text{Ag}^{107}(\alpha,n)$ reaction was undertaken for several reasons. The Coulomb barrier for helium ions in this region of the periodic table is low enough to give sizeable reaction cross sections for helium ions of approximately 15 MeV. However, in the decay of excited nuclei of this atomic number, the Coulomb barrier is large enough to severely inhibit proton evaporation relative to neutron emission. In addition, this particular reaction has an $(\alpha,2n)$ threshold large enough to allow a study of the (α,n) reaction over several MeV of excitation energy. The odd Z -odd N character of In^{110} makes it reasonable to treat this nucleus with a Fermi-gas theory and eliminates the necessity for choosing a characteristic level in the shifted Fermi-gas theory.

In deducing the nuclear moment of inertia from the experimental isomer ratios, the spin-dependent level density is assumed to be given by¹⁻³

$$\rho(J,E) = \rho(0,E) (2J+1) e^{-(J+1/2)^2/2\sigma^2}. \quad (1)$$

The spin cutoff factor σ is related to the nuclear moment of inertia \mathcal{I} by

$$\sigma^2 = \mathcal{I}t/\hbar^2, \quad (2)$$

where t is the thermodynamic temperature. With the assumption that the reactions proceed by compound nucleus formation, the isomer ratios were calculated by procedures which have been outlined previously.⁴⁻⁸ It is the purpose of this paper to investigate the nuclear moment of inertia of excited In^{110} through a study of the spin cutoff factor σ which is determined from the isomer ratio data. Furthermore, the sensitivity of the moment of inertia to changes in various parameters used in the theoretical calculations is examined.

II. EXPERIMENTAL PROCEDURES

Irradiations for producing the desired reactions were performed with the Argonne constant frequency 60-in. cyclotron. This cyclotron accelerates helium ions to an energy of about 42.5 MeV. The helium-ion energies given in this report are in the laboratory system. The energy of the cyclotron beam was determined from range measurements using range-energy curves constructed from the data of Bichsel.⁹ The desired energy of reaction was obtained by degrading the helium ions

with aluminum foils. The targets were silver foils, $\frac{3}{4}$ in. in diameter and about 2 mg/cm² thick. Separated isotopes¹⁰ (99.6% Ag^{107} and 99.8% Ag^{109}) were used in all bombardments. Usually two silver foils were irradiated at different helium-ion energies by placing these foils behind a different number of aluminum foils. The target assembly consisted of an aluminum "Faraday cup" which contained the silver target foils and the aluminum degrading foils. This "Faraday cup" was used to measure the current of the helium ions on the target so that absolute cross sections as well as isomer ratios could be determined. Typical beam currents were about 0.10 μA , and targets were irradiated for a length of time from 1.0 to 18.2 min.

The amounts of In^{110} and In^{110m} produced in the reactions were determined by scintillation counting using a total absorption gamma-ray spectrometer. This counter has been described by Hansen¹¹ and is similar to other counters described in the literature.¹² It consists essentially of two NaI(Tl) crystals, 4 in. in diameter and 4 in. high, mounted face to face, $\frac{3}{8}$ in. apart, in a 6-in.-diam hole through the center of a plastic anti-Compton shield. This plastic scintillator, 24 in. in diameter and 24 in. high, is NE-102 brand phosphor supplied by Nuclear Enterprises Ltd. of Winnipeg, Canada. It is shielded by 2 in. of lead. The sample is introduced between the two NaI(Tl) crystals on a slide which is inserted through a slot in the plastic scintillator.

In operation the outputs of the preamplifiers of the two NaI(Tl) crystals are added and fed into an ANL model A-61 linear amplifier (cf. Fig. 1 for diagram of electronics). The A-61 linear amplifier output is fed into the analog to digital converter circuit of an RCL-256 channel analyzer which is operated in the delayed coincidence mode. The A-61 discriminator

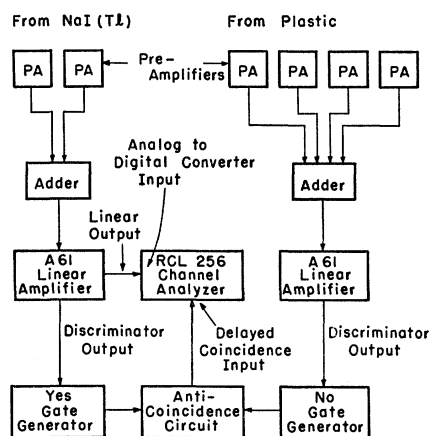


FIG. 1. Diagram of total absorption counter electronics.

¹ H. A. Bethe, Rev. Mod. Phys. **9**, 84 (1937).

² C. Bloch, Phys. Rev. **93**, 1094 (1954).

³ T. Ericson, Nucl. Phys. **11**, 481 (1959).

⁴ J. R. Huizenga and R. Vandenbosch, Phys. Rev. **120**, 1305 (1960).

⁵ R. Vandenbosch and J. R. Huizenga, Phys. Rev. **120**, 1313 (1960).

⁶ C. T. Bishop, Argonne National Laboratory Report 6405, 1961 (unpublished).

⁷ W. L. Hafner, Jr., J. R. Huizenga, and R. Vandenbosch, Argonne National Laboratory Report 6662, 1962 (unpublished).

⁸ H. K. Vonach, R. Vandenbosch, and J. R. Huizenga (to be published).

⁹ H. Bichsel, Phys. Rev. **112**, 1089 (1958).

¹⁰ Purchased from the Isotopes Division of Oak Ridge National Laboratory, Oak Ridge, Tennessee.

¹¹ N. Hansen, Argonne National Laboratory (unpublished results).

¹² W. H. Ellet and G. L. Brownell, Nucl. Instr. Methods **7**, 56 (1960).

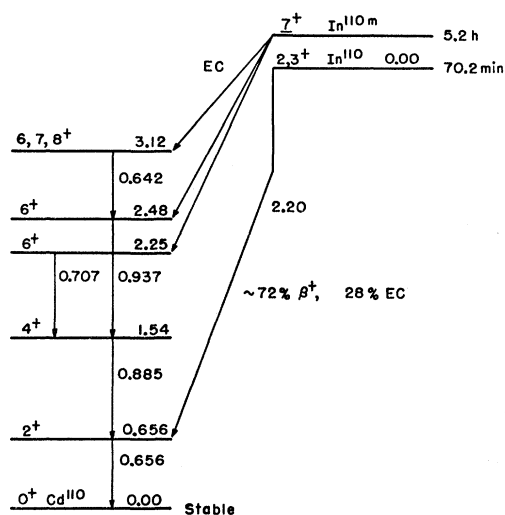


FIG. 2. Essential features of the In^{110} , In^{110m} decay schemes.

output is fed into a gate generator which generates a "yes" pulse, which in turn is fed into an anticoincidence circuit. The four outputs of the tubes viewing the plastic scintillator are added and fed into a second A-61 linear amplifier. The discriminator output from this amplifier is fed into a second gate generator which generates a "no" pulse. This "no" pulse is fed into the same anticoincidence circuit as was the "yes" pulse. Unless a "yes" and a "no" pulse occur simultaneously in the anticoincidence circuit, the "yes" pulse is fed into the delayed coincidence input of the RCL-256 channel analyzer, and causes the analyzer to process the pulse produced by the two NaI(Tl) crystals. When simultaneous pulses occur in both the NaI(Tl) crystals and in the plastic scintillator, the "no" pulse blocks the "yes" pulse in the anticoincidence circuit, and consequently the pulse produced by the two NaI(Tl) crystals is not analyzed or recorded. Thus, when a gamma ray is Compton scattered in one of the two NaI(Tl) crystals and escapes into the plastic scintillator, it is rejected, thereby reducing the Compton pulse-height distribution. This anticoincidence feature similarly reduces background due to cosmic radiation and natural radioactivity.

To determine the activity of the indium isomers the silver foils were counted directly, i.e., no chemical separations were necessary. An aluminum absorber of thickness 0.697 g/cm^2 was used on both sides of the sample. The essential features of the decay scheme for the isomeric pair In^{110} , In^{110m} are shown in Fig. 2.¹³⁻¹⁵ The half-lives given here have been determined by the present authors. The activity of the In^{110} was followed

¹³ *Nuclear Data Tables*, compiled by K. Way *et al.* (Printing and Publishing Office, National Academy of Sciences—National Research Council, Washington, D. C., 1959), NRC 60-2-75.

¹⁴ F. Katoh, M. Nozawa, and Y. Yoshizawa, *Nucl. Phys.* **32**, 25 (1962).

¹⁵ W. G. Smith, *Phys. Rev.* **124**, 168 (1961).

by measuring the intensity of its 656-keV gamma rays. In the above counter γ rays in coincidence with positrons will mainly appear in sum peaks, and hence such a counter records chiefly those 656-keV gamma rays following electron capture in In^{110} (this isomer decays about 28% by electron capture and about 72% by positron emission).¹³ It is more advantageous to measure the 656-keV gamma ray with a total absorption counter rather than with a single crystal because of the fact that less 656-keV gamma radiation due to In^{110m} is observed on the former counter. With the total absorption counter, greater than 95% of the 656-keV gamma radiation of In^{110m} will appear in a sum peak since its 656-keV gamma ray is in coincidence with 2 or 3 other gamma rays (cf. Fig. 2). Another advantage of the total absorption counter over a single crystal is the fact that less of the 511-keV gamma-ray peak, which overlaps slightly with the 656-keV peak, is observed with the total absorption counter. This is because of the fact that the 511-keV gamma rays from positron annihilation sum with each other and/or with the 656-keV gamma ray preceded by positron emission.

A typical gamma-ray spectrum of In^{110} is shown in Fig. 3. This is a spectrum of the irradiated silver foil about one hour after the end of the irradiation. Since higher energy peaks occur in this gamma-ray spectrum, it is necessary to subtract from the counts under the 656-keV peak those counts which are due to Compton distributions of higher energy peaks. Here again the use of a total absorption counter is advantageous because of its ability to reduce the intensity of the Compton distribution of the gamma-ray spectrum. This Compton distribution was subtracted from the 656-keV peak by extrapolation of the straight line portion of the spectrum on the right-hand side of this peak, under this peak, and subtracting out those counts falling under this line. Finally, in measuring the In^{110} activity, it was sometimes necessary to subtract from the 656-keV activity small contributions due to the presence of In^{109} and/or In^{110m} . (Recall that most of the 656-keV gamma radiation of In^{110m} will appear as sum peaks.) In^{109} , which is produced by the $\text{Ag}^{107}(\alpha, 2n)$ or the $\text{Ag}^{109}(\alpha, 4n)$

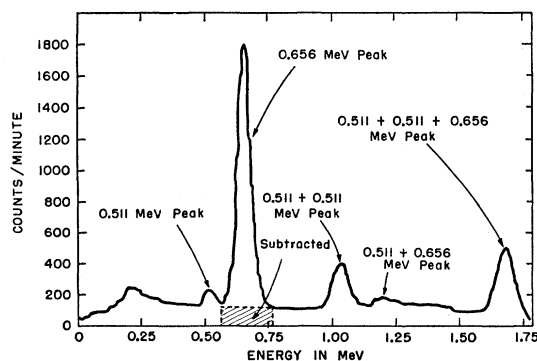


FIG. 3. Gamma-ray spectrum of In^{110} on the total absorption counter about one hour after irradiation.

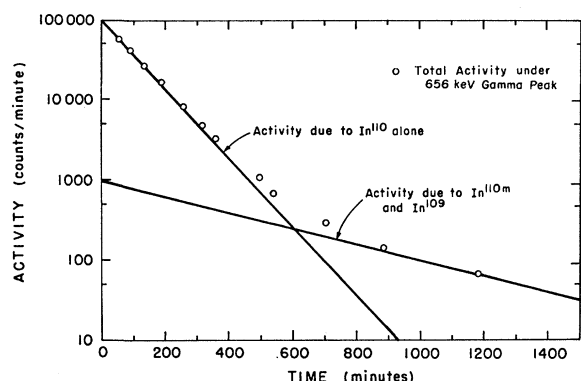


FIG. 4. Decay of the 656-keV gamma-ray activity observed in a Ag^{107} target bombarded with helium ions of an energy of 16.8–17.1 MeV.

reaction, has a 632-keV gamma ray which is unresolvable from the In^{110} 656-keV gamma ray. The In^{109} produced by these reactions will interfere considerably in the decay analysis when their reaction thresholds have been exceeded by a few MeV. The decay of a 656-keV gamma-ray peak is shown in Fig. 4 in which the bombarding helium-ion energy was 16.8–17.1 MeV. Most of the 656-keV activity at this energy was due to the In^{110} produced in the $\text{Ag}^{107}(\alpha, n)$ reaction. However, at the end of the irradiation, about 1% of the 656-keV peak was due to In^{110m} and to In^{109} . The threshold for the $\text{Ag}^{107}(\alpha, 2n)\text{In}^{109}$ reaction is 16.3 MeV.

The intensity of a sum peak of 3.12 MeV, as observed on the total absorption counter, was used to measure the In^{110m} activity. This sum peak is due to the sum of four gamma rays (cf. Fig. 2). A gamma-ray spectrum of the silver foil about 12 h after the end of the irradiation is shown in Fig. 5. The intensity of the 3.12-MeV peak was not too great, but because of the 5.2-h half-life of In^{110m} , a large number of counts could be accumulated by counting for a long period of time. Also because of the high energy of this peak, the background was only

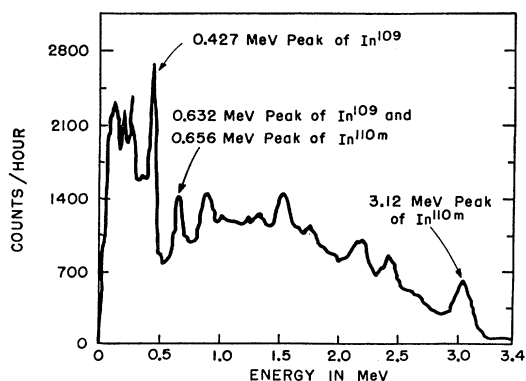


FIG. 5. Gamma-ray spectrum of In^{110m} recorded with the total absorption counter about 12 h after the end of a Ag^{107} bombardment with helium ions.

about 4 counts per minute compared to about 50 counts per minute in the channels containing the 656-keV peak. Another advantage to determining the activity of In^{110m} by measuring the intensity of the 3.12-MeV peak is the fact that at such a high energy there is little chance of contamination from other radioactivities which may be present in the sample.

To obtain the isomer ratio from the activities of the two In^{110} isomers, it was necessary to determine the counting efficiencies of the total absorption counter. This also made it possible to obtain absolute cross sections for the formation of each isomer. The counting efficiencies were determined experimentally by obtaining samples of In^{110} and of In^{110m} whose absolute disintegration rates had been determined by other means, and then counting these samples directly with the total absorption counter. A sample of In^{110} containing only a small amount of In^{110m} was prepared by irradiation of a Ag^{107} foil at a helium-ion energy of 12.4 MeV. As will be seen later, at this low energy little In^{110m} relative to In^{110} is produced. The absolute disintegration rate of the In^{110} sample was determined by counting the 656-keV gamma ray with a single 3-in. \times 3-in. NaI(Tl) crystal. It is assumed on the basis of the decay scheme of In^{110} that every In^{110} nucleus decays through the 656-keV excited state of Cd^{110} , and that the fractional decay of this level by electron conversion is negligible.¹³

Any 656-keV gamma radiation due to In^{110m} was subtracted. The In^{110m} contribution to the peak was observed by following the decay of the 656-keV gamma peak for several half-lives. The efficiency of the 3-in. \times 3-in. NaI(Tl) crystal was determined by use of a Cs^{137} intensity standard. Cs^{137} has a single gamma ray of 662 keV in its decay, and the absolute disintegration of this standard was determined by 4 π beta counting. The efficiency for counting the 656-keV gamma-ray photopeak of In^{110} with the total absorption counter was determined to be 9.52%.

A sample of In^{110m} containing only a trace of In^{110} was prepared by irradiation of a Ag^{107} foil at a helium-ion energy of 13.7 MeV, and then allowing the In^{110} to decay for about ten half-lives. This sample was counted in a 5-in. \times 5-in. NaI(Tl) well crystal using a single-channel analyzer which counted all pulses with energy greater than 8 keV. In such a counting arrangement, In^{110m} produces very close to one count per disintegration. This is true because for practically every disintegration of In^{110m} at least three gamma rays occur in cascade (cf. Fig. 2) and the probability that at least one of these gamma rays be detected by a 5-in. \times 5-in. NaI(Tl) crystal was calculated⁶ to be 0.993. Also, no isomeric transition of In^{110m} to In^{110} has been observed¹⁵ so that to a very good approximation the counting rate recorded by the 5-in. \times 5-in. NaI(Tl) crystal is equal to the In^{110m} disintegration rate. A very small amount of In^{111} , produced by the (α, γ) reaction on Ag^{107} , was found to be present in the In^{110m} sample. In^{111} emits gamma rays in its decay and has a half-life of 2.8 days. The

activity due to the In^{111} was determined by observing the counting rate of the irradiated silver foil over a period of several days, and then subtracting this activity from the total activity. The cross sections for the $\text{Ag}^{107}(\alpha, \gamma)\text{In}^{111}$ reaction for helium ions of 12.2 and 13.6 MeV were measured to be 0.5 ± 0.2 and 0.6 ± 0.2 mb, respectively. The efficiency for determining the disintegration rate of In^{110m} by measuring the 3.12-MeV gamma-ray photopeak with the total absorption counter was determined to be 1.02%.

III. EXPERIMENTAL RESULTS

The experimental cross-section ratios of the independently decaying isomers In^{110} and In^{110m} were calculated from the following equation,⁶

$$\frac{\sigma_2}{\sigma_1} = \frac{\lambda_2 N_2 (1 - e^{-\lambda_1 t})}{\lambda_1 N_1 (1 - e^{-\lambda_2 t})}. \quad (3)$$

The subscripts 1 and 2 refer to In^{110m} and In^{110} , respectively, σ is the cross section, λN is the disintegration

TABLE I. Experimental isomer ratios.

$\text{Ag}^{107}(\alpha, n)$ Reaction		$\text{Ag}^{109}(\alpha, 3n)$ Reaction	
Helium-ion energy (MeV)	$\sigma_{\text{In}^{110m}}$	Helium-ion energy (MeV)	$\sigma_{\text{In}^{110m}}$
	$\sigma_{\text{In}^{110m}} + \sigma_{\text{In}^{110}}$		$\sigma_{\text{In}^{110m}} + \sigma_{\text{In}^{110}}$
10.6–11.0	0.131	27.5–27.8	0.675
11.9–12.3	0.167	29.2–29.5	0.726
13.4–13.7	0.216	31.0–31.3	0.778
14.85–15.15	0.303	33.1–33.4	0.807
16.8–17.1	0.397	35.1–35.3	0.832
18.5–18.8	0.546	36.8–37.0	0.852
20.1–20.35	0.749	38.6–38.75	0.874
20.3–20.55	0.740		
21.8–22.1	0.807		

rate of the isomer after an irradiation time t , and λ is the decay constant of the isomer. To use this equation the disintegration rates of the isomers must be determined from their activities in the same irradiated target. Also a constant flux of the bombarding particles is assumed in the derivation of this equation. Actually there are slight fluctuations in the beam current during an irradiation ($\pm 20\%$), but as long as the length of the irradiation is short compared to the half-life of the shortest lived isomer, the above equation is valid to a very good approximation (irradiation times were usually 2, 3, or 4 min and the longest was 18.2 min).

The isomer ratios computed from the experimental data are given in Table I. The helium-ion bombarding-energy ranges given in this table refer to the average energy of the helium ion upon entering and upon leaving the silver foil. The difference is due to the finite thickness of the silver foil. The helium-ion beam at full energy of about 42 MeV actually has an energy spread, i.e., the full width at half-maximum beam intensity, of about 0.4 MeV. This spread will increase when the beam

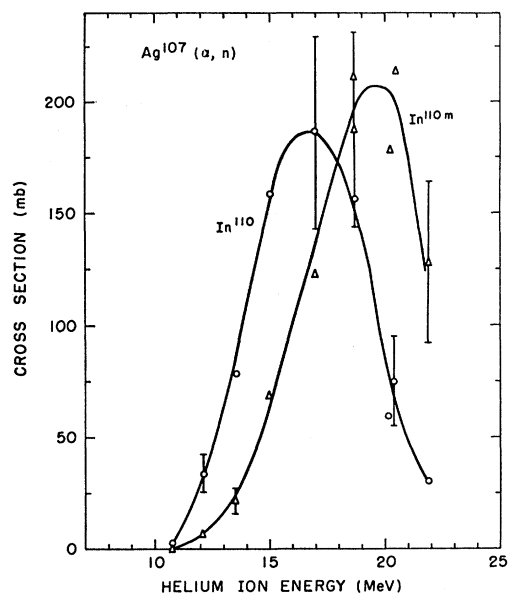


FIG. 6. Excitation functions for the $\text{Ag}^{107}(\alpha, n)\text{In}^{110}$ and $\text{Ag}^{107}(\alpha, n)\text{In}^{110m}$ reactions.

is degraded because of scattering effects in the aluminum foils; the beam spread is about 0.8 MeV at a helium-ion energy of 15 MeV. The excitation functions for the formation of In^{110} and In^{110m} by the $\text{Ag}^{107}(\alpha, n)$ and the $\text{Ag}^{109}(\alpha, 3n)$ reactions are shown in Figs. 6 and 7. Both the absolute cross sections and the isomer ratios for the $\text{Ag}^{107}(\alpha, n)$ reaction are in agreement within experimental error with the results recently reported by Fukushima *et al.*¹⁶ Agreement of the present results for the $\text{Ag}^{109}(\alpha, 3n)$ reaction with the results of Otozai¹⁷ are not quite as good. However, natural targets were used in the experiments of Otozai.

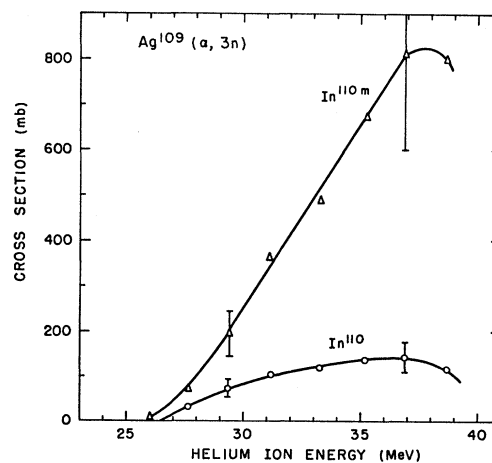


FIG. 7. Excitation functions for the $\text{Ag}^{109}(\alpha, 3n)\text{In}^{110}$ and $\text{Ag}^{109}(\alpha, 3n)\text{In}^{110m}$ reactions.

¹⁶ S. Fukushima, S. Hayashi, S. Kume, H. Okamura, K. Otozai, K. Sakamoto, and Y. Yoshizawa, Nucl. Phys. 41, 275 (1963).

¹⁷ K. Otozai (private communication).

The experimental $\text{Ag}^{107}(\alpha, n)$ and $\text{Ag}^{109}(\alpha, 3n)$ cross sections are compared with the theoretical total-reaction cross sections¹⁸ in Figs. 8 and 9, respectively. The leading side of the $\text{Ag}^{107}(\alpha, n)$ excitation function represents a major fraction of the total-reaction cross section. At helium-ion energies above 18 MeV, the $\text{Ag}^{107}(\alpha, 2n)$ reaction becomes dominant and the $\text{Ag}^{107}(\alpha, n)$ cross section drops sharply. The $\text{Ag}^{109}(\alpha, 3n)$ cross section peaks at about 38 MeV. However, even at this energy, a sizeable fraction of the reaction cross section goes into competing reactions such as $(\alpha, p2n)$, $(\alpha, 2n)$, $(\alpha, 4n)$, etc.

In determining the cross sections and cross-section ratios for the indium isomers a number of errors are involved:

- (1) Determination of In^{110} counting efficiency. These errors arise because of uncertainties in the decay schemes of In^{110} and Cs^{137} , and because of the rather indirect method of determining this efficiency: $\pm 6\%$.
- (2) Determination of In^{110m} counting efficiency: $\pm 4\%$.
- (3) Decay constants of In^{110} and In^{110m} : $\pm 2\%$ each.
- (4) Gamma-ray spectrum analysis. This error is greatest at the lowest and highest helium-ion energies of each reaction, because at these energies activities from competing reactions make the analysis of the gamma-ray spectrum more difficult: $\pm 3\%$ to $\pm 8\%$.
- (5) Miscellaneous small errors, e.g., inability to reproduce exact geometry: $\pm 2\%$.
- (6) Weight of silver target: $\pm 1.5\%$.
- (7) Current on target: $\pm 4\%$.

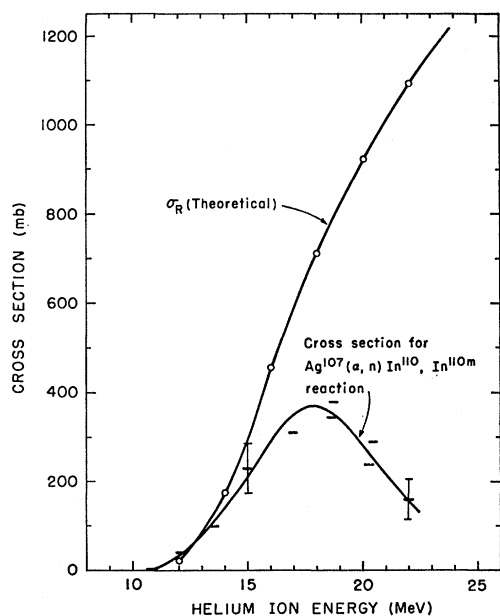


FIG. 8. Cross sections for the $\text{Ag}^{107}(\alpha, n)$ reaction are compared with theoretical optical-model reaction cross sections.

¹⁸ J. R. Huizenga and G. J. Igo, Nucl. Phys. **29**, 473 (1962); Argonne National Laboratory Report 6373, 1961 (unpublished).

The over-all error in the determination of the individual cross sections may be as high as 28%. However, the isomer ratios are of primary interest, and since Eq. (3) was used in the determination of these ratios, the last two errors above do not enter into the error of the isomer ratio. Also, since these ratios were measured at a number of helium-ion energies, it is meaningful to consider constant and random errors. Of the errors listed above the first three were constant for each measurement of the cross-section ratio, while the fourth and fifth were random in nature. Table II gives some examples of the errors involved in the isomer ratios at various helium-ion energies. These errors are maximum errors obtained by adding all of the errors involved in the experimental determination of the isomer ratio. In addition to the errors involved in the activity determinations, there are errors in the measurement of the energy of the helium ions. The error in measuring the

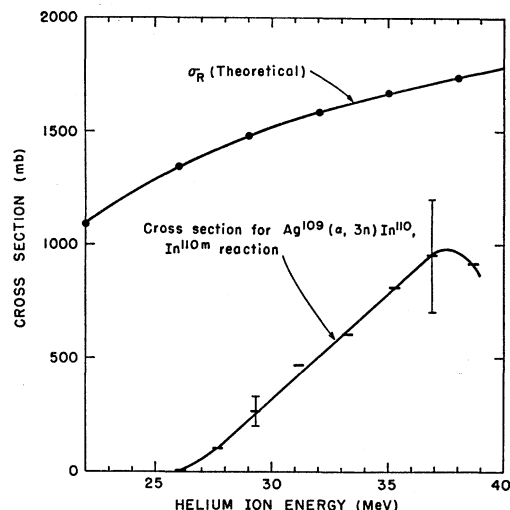


FIG. 9. Cross sections for the $\text{Ag}^{109}(\alpha, 3n)$ reaction are compared with theoretical optical-model reaction cross sections.

helium-ion bombarding energy from range measurements was about $\pm 2\%$ at 38 MeV and was as high as $\pm 10\%$ at 12 MeV.

IV. THEORETICAL CALCULATION METHODS

The method used to calculate the theoretical isomer ratios for the Fermi-gas model has been described elsewhere.^{4,5} Additional details for the In^{110} isomers are available in a separate report.⁶ The calculations were performed on an IBM-704 computer.⁷ Transmission coefficients for the bombarding helium ions and evaporated neutrons were calculated with a revised version Abacus II optical-model program.¹⁹ The optical-model

¹⁹ The authors are indebted to E. H. Auerbach and C. E. Porter for supplying this program.

parameters used in the computations were taken from the literature.^{18,20}

The calculation assumes the reaction mechanism to be compound nucleus formation. The excitation energy of the initial compound nucleus E_C is equal to the binding energy of the incoming particle B plus its kinetic energy in center-of-mass coordinates, $E_C = B + E_{CM}$. Following neutron emission the average energy of the residual nucleus, E_r , is given by $E_r = E_C - B_n - \bar{E}_n$, where E_C is the initial compound-nucleus excitation energy, B_n is the binding energy of the outgoing neutron, and \bar{E}_n is the average energy of the emitted neutrons. In most calculations an average neutron energy of twice the nuclear temperature was assumed. In addition, we assumed the nuclear temperature T to be related to the excitation energy E by²¹

$$E = aT^2 - 4T, \quad (4)$$

where a is the level density parameter.

The average excitation energy of a residual nucleus following gamma-ray emission was computed by assuming that the average energy of the dipole gamma ray emitted from a nucleus of initial excitation energy E is given by⁸

$$\bar{E}_\gamma = 4[(E/a) - (5/a^2)]^{1/2}. \quad (5)$$

The energy of each succeeding gamma ray in the cascade is found by computing the new initial excitation energy and the use of Eq. (5). Some arbitrariness is introduced into the calculation by the choice of excitation energy at which the isomer deciding transition (may be of any multipolarity) takes place. The following choice was adopted for the energy of the final γ ray. If a γ -ray transition leads to an excitation energy below 1 MeV, only the deciding γ ray is emitted. If a γ -ray transition leads to an excitation energy greater than 2 MeV, the next γ -ray transition will not contain any of the deciding γ -ray transition. If a γ -ray transition leads to an excitation energy E between 1 and 2 MeV, there is a probability $(2-E)$ that the deciding γ ray is emitted and a probability $(E-1)$ that one γ ray precedes the deciding γ ray. This assumption about the γ -ray cutoff in conjunction with Eq. (5) gives a theoretical number of γ rays from neutron capture in reasonable agreement with the experimental measurements of the average number of γ rays \bar{N}_γ per neutron capture. As these measurements, however, show rather large fluctuations in \bar{N}_γ for neighboring nuclei, the influence of such deviations in the number of γ rays on the results of the calculations has been investigated.

As mentioned previously the deciding γ ray may have multipolarity greater than one. If the ground-state spin of In^{110} is assumed to be 2 (the isomeric state has been measured to be 7),¹³ and P_{J_f} represents the absolute

TABLE II. Sample errors in isomer ratios for $\text{Ag}^{107}(\alpha, n)$ and $\text{Ag}^{109}(\alpha, 3n)$ reactions.

Helium-ion energy (MeV)	$\frac{\sigma_{\text{In}^{110m}}}{\sigma_{\text{In}^{110}} + \sigma_{\text{In}^{110m}}}$	Constant error	Random error
11.9-12.3	0.167	± 0.021	± 0.007
16.8-17.1	0.397	± 0.036	± 0.015
21.8-22.1	0.807	± 0.023	± 0.015
27.5-27.8	0.675	± 0.033	± 0.022
33.1-33.4	0.807	± 0.023	± 0.013
38.6-38.75	0.874	± 0.017	± 0.011

probability that the nucleus will have a spin J_f before the emission of the last gamma ray, then

$$\frac{\sigma_{\text{In}^{110m}}}{\sigma_{\text{In}^{110m}} + \sigma_{\text{In}^{110}}} = \sum_{J_f=5}^{\infty} P_{J_f}. \quad (6)$$

If the spin of the ground-state isomer is 3, one assumes in the calculation that the spin 5 states divide equally in the final γ -ray transition between the two isomers.

The nuclear-spin density parameter σ [not to be confused with the cross section of Eq. (3)] is related to the nuclear moment of inertia by Eq. (2). For a square mass distribution the rigid-body moment of inertia is given by²²

$$I_{\text{rigid}} = \left(\frac{2}{5}\right)mAR^2, \quad (7)$$

where m is the nucleon mass, A the number of nucleons, and R the nuclear radius. The radius is assumed to be equal to $r_0 A^{1/3}$ where $r_0 = 1.2 \times 10^{-13}$ cm. The relationship between the thermodynamic temperature and excitation energy is given by the equation²¹

$$E = at^2 - t. \quad (8)$$

The calculations were performed for various values of the level density parameter a . In most of the calculations the rigid-body moment of inertia was used. The energy dependence of σ is introduced through the relationship given in Eq. (8). However, for an odd Z -odd N nucleus such as In^{110} the value of σ must be finite even for zero excitation energy. In these calculations we have assumed the following lower limit for σ :

$$\sigma^2 \geq 2\langle m^2 \rangle, \quad (9)$$

where $\langle m^2 \rangle$ is the mean square value of the magnetic quantum number of an excited nucleon. Furthermore, the term $\langle m^2 \rangle$ was evaluated from the relationship²²

$$\langle m^2 \rangle g = I_{\text{rigid}} / \hbar^2, \quad (10)$$

where g is the number of single-particle levels per MeV (for protons and neutrons) and equal²¹ to $6a/\pi^2$, a being the more familiar level density parameter. The evaluation of the lower limit of σ by this method is only a crude approximation, since the exact value is expected to be shell-dependent.

²⁰ E. J. Campbell, H. Feshbach, C. E. Porter, and V. F. Weisskopf, Atomic Energy Commission Report TID-5820, 1960 (unpublished.)

²¹ D. W. Lang, Nucl. Phys. **43**, 353 (1963).

²² T. Ericson, Advan. Phys. **9**, 425 (1960).

V. THEORETICAL CALCULATION RESULTS AND DISCUSSION

A. Approximation of Neutron Energy Spectrum by an Average Neutron Energy of $2T$

Computations were performed to test the sensitivity of the results of the isomer calculations to the assumption that the neutron spectrum is treated as a monoenergetic line of energy $2T$. In these comparisons a theoretical neutron spectrum is divided into several bins and each energy bin is processed separately. The results of such a calculation for the $\text{Ag}^{107}(\alpha, n)$ reaction with 16-MeV helium ions are given in Table III. The neutron energy spectrum was computed with a level density parameter $a=15 \text{ MeV}^{-1}$. The energy range of the neutron bins and their intensities are listed in Table III. As can be seen in Table III, the isomer ratio is rather independent of neutron energy and the weighted average of all bins is equal to the value calculated for neutron energy of $2T$. A larger value of N_γ is associated with smaller neutron energies, and the combined effect of changing the neutron energy and the number of γ rays gives a rather constant isomer ratio. Since the calculated isomer ratios are very insensitive to neutron energy, the exact form of the level density and the expression used in computing the neutron spectrum are expected to be unimportant for this calculation.

B. Calculations for the $\text{Ag}^{107}(\alpha, n)$ Reaction

Calculations of the isomer ratios for the $\text{Ag}^{107}(\alpha, n)$ $\text{In}^{110,110m}$ reaction were carried out for helium-ion energies between 12 and 22 MeV. Nuclear level density parameters of 10, 15, and 25 MeV^{-1} were used in computing the ratios. From experimental neutron spectra obtained in (n, n') reactions²³⁻²⁶ and (p, n) reactions,²⁷

TABLE III. Calculation of the isomer ratio as a function of neutron energy for $\text{Ag}^{107}(\alpha, n)$ at a helium-ion energy of 16 MeV. A level density parameter a of 15 MeV^{-1} was used in computing the spectrum. For this calculation $2T=1.54 \text{ MeV}$.

Energy range of bin (MeV)	Relative weight of bin	Ave. neutron energy of bin (MeV)	N_γ^a	$\sigma_{\text{In}^{110m}}$
				$\sigma_{\text{In}^{110m}} + \sigma_{\text{In}^{110}}$
0	0.163	0.30	4.0	0.455
0.50-0.80	0.144	0.65	4.0	0.450
0.80-1.20	0.189	1.00	3.9	0.448
1.20-1.90	0.235	1.54	3.6	0.451
1.90-2.30	0.087	2.10	3.3	0.455
2.30-3.40	0.126	2.85	3.0	0.455
3.40-7.37	0.056	4.10	2.5	0.438

^a This is the average number of gamma rays emitted by the nucleus after emission of a neutron having an energy equal to the average neutron energy of the given bin.

^b The weighted average of all seven bins is 0.451.

²³ D. B. Thomson, Phys. Rev. **129**, 1649 (1963).

²⁴ S. G. Buccino, C. E. Hollandsworth, H. W. Lewis, and P. R. Bevington, Nucl. Phys. (to be published).

²⁵ K. J. LeCouteur and D. W. Lang, Nucl. Phys. **13**, 32 (1959).

²⁶ K. K. Seth, *Proceedings of the Conference on Direct Interactions*

and a of 15 MeV^{-1} seems reasonable for nuclei in the vicinity of In^{110} . However, calculations were also performed for $a=25 \text{ MeV}^{-1}$ and $a=10 \text{ MeV}^{-1}$ which appear to be upper and lower limits for the nuclear level density parameter in the mass region of In^{110} .

For the Fermi-gas calculations, the spin cutoff factor σ was computed with Eqs. (2), (7), and (8). The γ -ray cascade was treated as described in Sec. IV. However, some calculations were made with a γ -ray cutoff of 0.5-1.50 MeV instead of the 1.0-2.0-MeV cutoff described in Sec. IV. This in effect adds about $\frac{1}{2}$ γ ray per cascade. From Table IV, it can be seen that the calculated isomer ratios are insensitive to changes in the γ -ray cutoff. However, the small differences resulting from the two assumptions about the γ -ray cutoff are slightly accentuated for larger values of a .

For helium-ion bombarding energies where a neutron energy of $2T$ gives an excitation energy exceeding the next neutron binding energy, some modification of the assumption that the average neutron energy equals $2T$ is necessary. In these cases the assumption was usually made that neutrons were of sufficient energy to lead to an excitation energy in the residual nucleus equal to its neutron binding energy. As pointed out in Sec. V.A, this uncertainty in neutron energy was not a problem since the calculated isomeric ratios are very insensitive to the choice of neutron energy.

The experimental isomer ratios are compared with the theoretical ratios for a Fermi-gas model in Fig. 10. Although the isomeric state has a measured spin of 7, the ground-state spin is inferred from decay scheme data to be 2 or 3.¹³ The calculations presented in Fig. 10 assume the ground-state spin to be 2. Below a helium-ion energy of 18 MeV [the energy at which the $(\alpha, 2n)$ competition begins] the slopes of the experimental and all theoretical curves are in good agreement. The absolute values of the theoretical curve for $a=25 \text{ MeV}^{-1}$ agree with the experimental data. In order to obtain agreement between experiment and theory for $a=15 \text{ MeV}^{-1}$, the moment of inertia has to be reduced

TABLE IV. Comparison of theoretical isomer ratios for the $\text{Ag}^{107}(\alpha, n)\text{In}^{110,110m}$ reaction for $a=15 \text{ MeV}^{-1}$ and two different assumptions about the γ -ray cutoff (see Sec. IV).

Helium-ion energy (MeV)	$\sigma_\gamma/(\sigma_\gamma + \sigma_\alpha)$	
	1.00-2.00 MeV γ -ray cutoff	0.50-1.50 MeV γ -ray cutoff
12	0.201	0.194
14	0.293	0.287
16	0.451	0.433
18	0.606	0.581
20	0.685	0.662
22	0.736	0.727

and *Nuclear Reaction Mechanisms, Padua, Italy, September, 1962* (Gordon and Breach Publishers, New York, 1963), p. 267.

²⁷ R. L. Bramblett and F. W. Bonner, Nucl. Phys. **20**, 395 (1960).

to approximately $\frac{3}{4}$ of the rigid-body moment. However, if the ground state has spin 3, experiment and theory are in good agreement for $a=15 \text{ MeV}^{-1}$ in conjunction with the rigid-body moment of inertia as displayed in Fig. 11.

The theoretical calculations for the $\text{Ag}^{107}(\alpha, n)$ reaction were also performed with a superconductor model which is developed in some detail in another publication.⁸ For the odd Z -odd N nucleus In^{110} , this model gives values of the spin cutoff parameter σ which are 10–15% smaller than those deduced from the Fermi-gas model. Hence, with the superconductor model, good agreement is attained between experiment and theory for $a=15 \text{ MeV}^{-1}$ and a ground-state spin of 2 (Fig. 12). From this calculation one may conclude that the two models give quite similar results for odd Z -odd N nuclei. However, if the ground-state spin of In^{110} were measured, the experimental results might slightly favor one model over the other. A ground-state spin of 3 favors a rigid-body moment of inertia, whereas a spin of 2 favors a slightly reduced (by $\sim 25\%$) moment of inertia.

C. Influence of $(\alpha, 2n)$ Competition on Isomer Ratios from an (α, n) Reaction

In Figs. 10–12 one sees that for helium-ion energies greater than 18 MeV the slopes of the experimental and theoretical isomer ratios diverge markedly. This is approximately the helium-ion energy where the $(\alpha, 2n)$ reaction becomes probable (threshold energy of 16.2 MeV plus $2T$). Following neutron emission, residual nuclei with approximately 8 MeV of excitation energy can decay by either the emission of a second neutron [giving an $(\alpha, 2n)$ reaction], or by gamma emission²⁸ to a level below the neutron binding energy [giving an (α, n) reaction]. With the energy-dependent spin cutoff

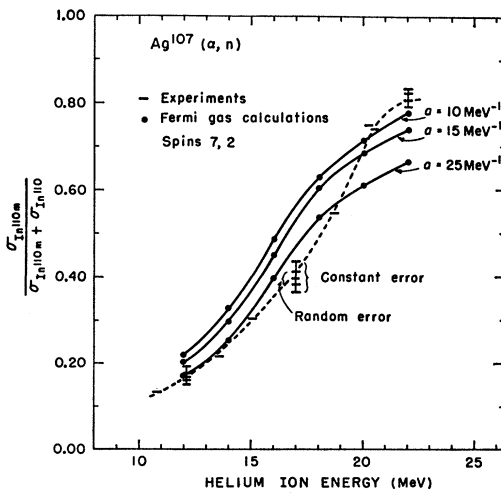


FIG. 10. Fermi-gas theoretical isomer ratios for various values of the nuclear level-density parameter a are compared with experimental values for the $\text{Ag}^{107}(\alpha, n)\text{In}^{110, 110m}$ reaction.

²⁸ J. R. Grover, Phys. Rev. **127**, 2142 (1962).

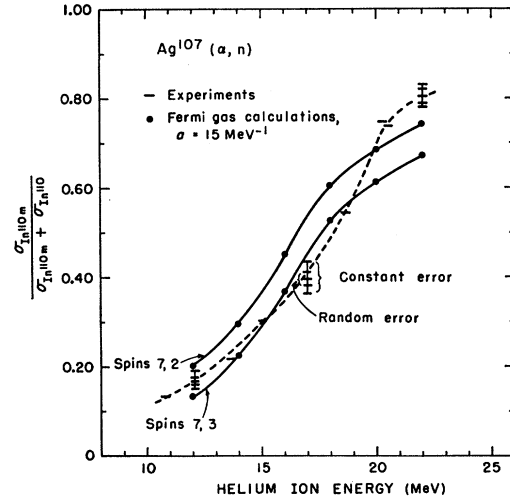


FIG. 11. Comparison of the experimental and Fermi-gas theoretical isomer ratios for the $\text{Ag}^{107}(\alpha, n)\text{In}^{110, 110m}$ reaction for In^{110} ground-state spins of 2 and 3.

factor σ predicted by either the Fermi-gas or superconductor models, one expects near threshold that the spin distribution leading to gamma emission will have a larger abundance of high-spin states than will the spin distribution leading to neutron emission. This fractionation of the spin spectrum results in an enhanced isomer ratio for the $\text{Ag}^{107}(\alpha, n)$ reaction, which is indeed the observed effect. Approximate calculations of the magnitude of this effect are in progress.²⁹ An alternative explanation of the large isomer ratios at the highest bombarding energies requires a moment of inertia exceeding the rigid-body moment, and hence is unlikely.

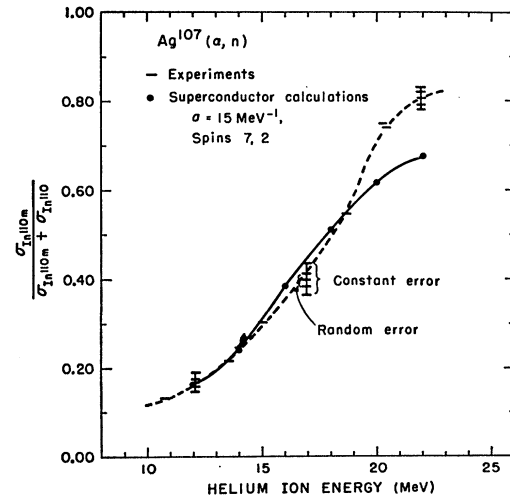


FIG. 12. Comparison of experimental and superconductor theoretical isomer ratios for the $\text{Ag}^{107}(\alpha, n)\text{In}^{110, 110m}$ reaction.

²⁹ J. C. Norman, L. Haskin, and J. R. Huizenga (private communication).

D. Calculations for the $\text{Ag}^{109}(\alpha, n)$ Reaction

The calculations of the isomer ratio for this reaction are essentially the same as those for the $\text{Ag}^{107}(\alpha, n)$ reaction except for the fact that the In^{112} isomers have different spins than those of the In^{110} isomers.¹³ The calculated isomer ratios for $\text{Ag}^{109}(\alpha, n)\text{In}^{112,112m}$ are compared with the experimental results of Otozai in Fig. 13. Unfortunately, the spins of neither isomer have been measured. Decay scheme data³⁰ indicate that the ground state (12-min activity) of In^{112} has a spin of 1, and a 21-min isomeric state has a spin of at least 4. The calculated isomer ratios for spin combinations of (4,1) and (5,1) are shown in Fig. 13. The calculated ratios are not unique for a particular pair of spins. For example, spins of (6,0) and (4,2) would give the same theoretical isomer ratios as spins of (5,1). Although the data do not allow one to assign spin values to the isomers of In^{112} , one can definitely conclude that the value of $(J_m + J_g)/2$ for the In^{112} isomers is at least 2 units smaller than the comparable quantity for In^{110} . Again in the neighborhood of 15 MeV, the experimental and theoretical isomer ratios diverge. This may again be due to $(\alpha, 2n)$ competition since the threshold for this reaction on Ag^{109} is 2 MeV less than for Ag^{107} . The leveling off of the isomer ratios at high helium-ion energies for both the $\text{Ag}^{107}(\alpha, n)$ and $\text{Ag}^{109}(\alpha, n)$ reactions is probably associated with the occurrence of a direct reaction mechanism at these energies.

E. Calculations for the $\text{Ag}^{109}(\alpha, 3n)$ Reaction

Calculations of the isomer ratio for the $\text{Ag}^{109}(\alpha, 3n)\text{In}^{110,110m}$ reaction were made for helium-ion energies between 26 and 38 MeV. Calculations were performed for a Fermi-gas model with a rigid-body moment of inertia and two values of the level density parameter, $a = 15$ and 25 MeV^{-1} . At the lower helium-ion energies,

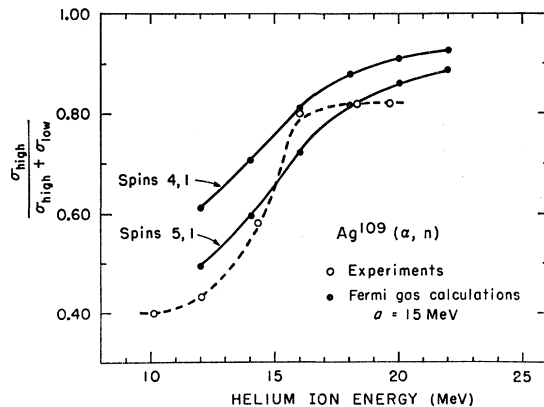


FIG. 13. Fermi-gas theoretical isomer ratios for the $\text{Ag}^{109}(\alpha, n)\text{In}^{112,112m}$ reaction with isomer spins of (4,1) and (5,1). The experimental data are those of Otozai (Ref. 17).

³⁰ J. Ruan, Y. Yoshizawa, and Y. Koh, Nucl. Phys. 36, 431 (1962).

the $(\alpha, 3n)$ reaction is energetically possible only when the evaporated neutrons fall in the low-energy part of the various neutron spectra. In these cases it is therefore appropriate to use neutron energies which are less than $2T$. However, the choice of energy for each of the three neutrons is somewhat arbitrary. Fortunately, the theoretical isomer ratios are insensitive to variations in the average neutron energy. For example, the $a = 15 \text{ MeV}^{-1}$ and a helium-ion energy of 29 MeV is 0.872 when the average neutron energies are 1.25, 1.11, and 0.50 MeV for the first, second, and third neutron, respectively. When these average neutron energies are changed to 0.75, 0.50, and 0.25 MeV, respectively, the calculated isomer ratio is 0.871.

A comparison of the experimental and calculated isomer ratios for the $\text{Ag}^{109}(\alpha, 3n)$ reaction is shown in Fig. 14. Near the peak cross section of the $(\alpha, 3n)$ reaction at about 38 MeV, the experimental and the-

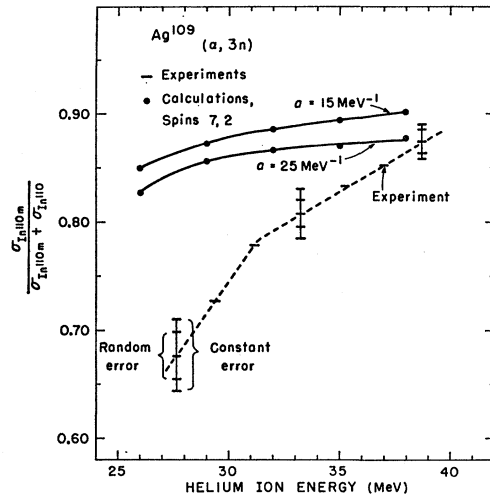


FIG. 14. Fermi-gas theoretical isomer ratios for the $\text{Ag}^{109}(\alpha, 3n)\text{In}^{110,110m}$ reaction compared with experimental ratios.

oretical isomer ratios are in agreement. As the helium-ion energy is reduced, the theoretical ratios become increasingly larger than the experimental ratios. This result is consistent with that expected if the spin distribution of states giving rise to the third emitted neutron is fractionated. This effect has already been discussed in Sec. V.C. However, the isomer ratio from an $(\alpha, 3n)$ reaction is reduced when the $(\alpha, 2n)$ competes strongly. On the other hand, the isomer ratio from an $(\alpha, 3n)$ reaction is enhanced when the $(\alpha, 4n)$ reaction competes strongly. At the peak of the $(\alpha, 3n)$ excitation function, the influence of the $(\alpha, 2n)$ and $(\alpha, 4n)$ competition on the spin distribution should cancel to first order. Therefore, for reactions in which several particles are emitted, it is reasonable to believe that the simple theory will have the best chance of reproducing the experimental data at energies where the excitation functions have maximum values.

The moment of inertia would have to be reduced considerably beyond the limits established from the (α, n) reaction in Sec. V.B in order to reduce the theoretical isomer ratios from the $(\alpha, 3n)$ reaction down to the experimental ratios obtained for 28–33-MeV helium ions. Such an argument supports the earlier suggestion that spin fractionation occurs for two competing reactions at energies near the threshold of one of the reactions, and hence, seriously alters the isomer ratio of each reaction.

F. Calculations for the $\text{Ag}^{107}(\alpha, 3n)$ Reaction

Again, to a good approximation the spin distributions calculated for the $\text{Ag}^{109}(\alpha, 3n)\text{In}^{110,110m}$ reaction represent the spin distributions for the $\text{Ag}^{107}(\alpha, 3n)\text{In}^{108,108m}$ reaction, and thus were used to calculate isomer ratios for the latter reaction. The threshold for the former reaction is at a helium-ion energy of 25.3 MeV, while the threshold for the latter reaction is 27.0 MeV. For the $\text{Ag}^{107}(\alpha, 3n)$ reaction it was more meaningful to compare the experimental and theoretical ratios of the cross section for the formation of the high-spin isomer to the cross section for the formation of the low-spin isomer, $\sigma_{\text{high}}/\sigma_{\text{low}}$, rather than values of the defined isomer ratio which is used in the rest of the text. Since the spins of In^{108} and In^{108m} are not certain, calculations of $\sigma_{\text{high}}/\sigma_{\text{low}}$ were computed for several pairs of spin values. The results of the theoretical calculations are shown in Fig. 15 along with the experimental ratios for the $\text{Ag}^{107}(\alpha, 3n)^{16}$ and $\text{Ag}^{109}(\alpha, 3n)$ reactions. The experimental points for $\text{Ag}^{107}(\alpha, 3n)$ reaction are plotted on the basis that the 40-min In^{108} activity is the low-spin isomer and the 58-min activity is the high-spin isomer. The difference in the slopes of the two experimental curves indicates that the sum of the isomer spins for In^{108} is less than the sum of the isomer spins for In^{110} . The calculated curve for each of the four pairs of spins passes through the experimental curve for the $\text{Ag}^{107}(\alpha, 3n)$ reaction, but the slope of each calculated curve differs by a fair amount from the experimental curve. This discrepancy between experiment and theory was discussed in Sec. V.E for an $(\alpha, 3n)$ reaction and explained on the basis that the theoretical calculations neglected the effect of spin fractionation. From the previous discussion on spin fractionation (Sec. V.E) one expects the best agreement between theory and experiment for an $(\alpha, 3n)$ reaction will be attained near the peak in its excitation function. Since there are rather large errors in the experimental $\sigma_{\text{high}}/\sigma_{\text{low}}$ ratios

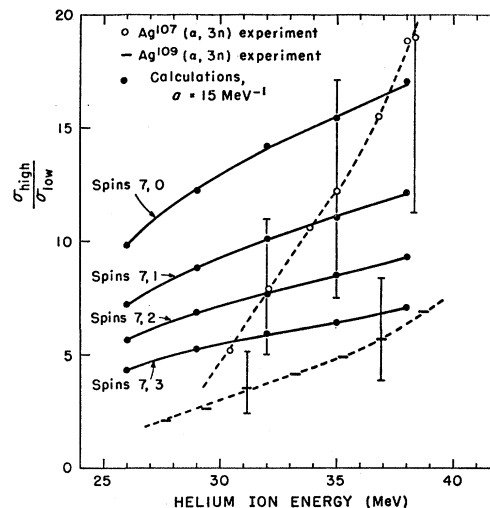


FIG. 15. Fermi-gas theoretical high-spin to low-spin cross-section ratios for various spin values of the isomers produced in the $\text{Ag}^{109}(\alpha, 3n)\text{In}^{110,110m}$ and the $\text{Ag}^{107}(\alpha, 3n)\text{In}^{108,108m}$ reactions compared with the experimental ratios. The experimental ratios for the $\text{Ag}^{107}(\alpha, 3n)$ reaction are those of Fukushima *et al.* (Ref. 16). The calculated ratios for spins (7,0) are identical with those of spins (6,1), (5,2), etc. Similarly the other calculated curves correspond to other spin pairs.

for the $\text{Ag}^{107}(\alpha, 3n)$ reaction near the peak in the excitation function, the experimental data overlap the theoretical values designated by spins (7,1) in Fig. 15. If the experimental value at 38 MeV is as small as that represented by the lower error bar, the $\sigma_{\text{high}}/\sigma_{\text{low}}$ ratios are consistent with the spins of 6 and 2 assigned for In^{108} isomers by decay scheme³¹ analysis.

It should be remembered that the calculations do not distinguish between the following pairs of spins, (7,1), (6,2), and (5,3). However, the theoretical values of $\sigma_{\text{high}}/\sigma_{\text{low}}$ designated by spins (7,0) are in better agreement with experiment. Again, the calculations are identical for spin pairs (7,0), (6,1), (5,2), etc. The decay-scheme evidence for the assignment of spin 2 or 3 to the 40-min isomer of In^{108} is considerably better than the evidence for assignment of spin value 6 or 7 to the 58-min isomer. A best estimate of the isomer spins of In^{108} from the $\sigma_{\text{high}}/\sigma_{\text{low}}$ ratios and decay-scheme analysis is 2 and 5, although other values are consistent with the large uncertainties in the experimental data. This analysis is based on two isomers and is not valid if a third isomeric state exists.

³¹ T. Katoh, M. Nozawa, and Y. Yoshizawa, Nucl. Phys. **36**, 394 (1962).